In Situ Metalorganic Deposition of Silver Nanoparticles on Gold Substrate and Square Wave Voltammetry: A Highly Efficient Combination for Nanomolar Detection of Nitrate Ions in Sea Water

Emilie Lebon Tailhades, Pierre Fau, Maurice Comtat, Myrtil L. Kahn, Alix Sournia-Saquet, Pierre Temple-Boyer, Brigitte Dubreuil, Philippe Behra, Katia Fajerwerg

chemosensors

MDPI

Communication

In Situ Metalorganic Deposition of Silver Nanoparticles on Gold Substrate and Square Wave Voltammetry: A Highly Efficient Combination for Nanomolar Detection of Nitrate Ions in Sea Water

Emilie Lebon [1,2], Pierre Fau [1,3,*], Maurice Comtat [3,4], Myrtil L. Kahn [1], Alix Sournia-Saquet [1], Pierre Temple-Boyer [5], Brigitte Dubreuil [6], Philippe Behra [6] and Katia Fajerwerg [1,3,*]

1 Laboratoire de Chimie de Coordination, UPR 8241 CNRS, 205 Route de Narbonne, 31077 Toulouse Cedex 4, France; emilie.lebon@airbus.com (E.L.); myrtil.kahn@lcc-toulouse.fr (M.L.K.); alix.sournia-saquet@lcc-toulouse.fr (A.S.-S.)
2 RTRA "Sciences et Technologies pour l'Aéronautique et l'Espace", F-31030 Toulouse, France
3 Université Paul Sabatier, UT III, 118 route de Narbonne, 31062 Toulouse Cedex 9, France; comtat@chimie.ups-tlse.fr
4 Laboratoire de Génie Chimique, UMR CNRS 5503, 118, route de Narbonne, 31062 Toulouse CEDEX 9, France
5 Laboratoire d'Analyse et d'Architecture des Systèmes (LAAS), 31400 Toulouse, France (CNRS); temple@laas.fr
6 Laboratoire de Chimie Agro-industrielle (LCA), Université de Toulouse, INRA, INPT, 31030 Toulouse Cedex 4, France; brigitte.dubreuil@ensiacet.fr (B.D.); philippe.behra@ensiacet.fr (P.B.)
* Correspondence: pierre.fau@lcc-toulouse.fr (P.F.); katia.fajerwerg@lcc-toulouse.fr (K.F.); Tel.: +33-5-613-33181 (P.F.); +33-5-613-33130 (K.F.)

Received: 13 August 2018; Accepted: 29 October 2018; Published: 6 November 2018

Abstract: The electro-reduction of nitrate ions in artificial sea water was investigated at a gold substrate (E_{Au}) functionalized by silver nanoparticles (AgNPs). These AgNPs were generated *in situ* on the gold substrate by the direct decomposition of the metalorganic N,N′-diisopropylacetamidinate silver precursor [Ag(Amd)] in the liquid phase. Very small and well dispersed AgNPs were deposited on the gold electrode and then used as working electrode ($E_{Au/AgNPs}$). Square wave voltammetry (SWV) was successfully employed to detect nitrate ions (NO_3^-) with a detection limit (LOD) of 0.9 nmol·L^{-1} in artificial sea water (pH = 6.0) without pre-concentration or pH adjustment.

Keywords: silver metalorganic precursor; silver nanoparticles; nitrate detection; square wave voltammetry; sea water

1. Introduction

Nitrate (NO_3^-) and nitrite (NO_2^-) ions are naturally present in soil, water, and food. They are important environmental and human health analytes [1,2] and their detection and measurement are essential.

In the oceanic environment, phytoplankton photosynthesis is in part controlled by major macronutrient elements such as nitrogen, phosphorous, and silicon. Nitrate is moreover of particular interest because it acts as a marker for water quality and represents the main source of nitrogen in marine ecosystems. High resolution measurements of nitrate are essential for the understanding of biogeochemical cycles in aquatic systems. Nitrate concentrations in natural waters range from the subnanomolar level in the oligotrophic open ocean because of the biological uptake, to the hundred micromolar level in rivers nearby to intensive agricultural activity. There are several procedures and many techniques reported in the literature for nitrate determination in continental [1] or sea water [3].

Among the analytical methods to measure the concentration of nitrates are capillary electrophoresis, chromatography, UV absorption, and so on [4]. Some of them require chemical reagents and/or necessitate complex and costly equipment [5]. In addition, most of them also require pre-treatment steps which are not compatible with a direct and *in situ* measurement of nitrates.

Comparatively, electrochemical sensing devices represent an interesting alternative to nitrate determination. The advantages of the electroanalytical techniques over other detection methods are many: low cost, ease of use, low energy requirements and simple procedures, and the possibility to build portable and miniaturized systems that are suitable either for laboratory assessments or on-site measurements.

The electrochemical reduction of NO_3^- has been performed for decades on several electrodes (Pt, Pd, Ni, Ru, Ag, Au, etc.) and is well known to be a very complex process [6]. These results were mainly focused to achieve high performances with high concentrations of nitrate ions in acidic or basic aqueous media which are not suitable for real measurements in sea water conditions, that is, subnanomolar levels and a pH range of 5.0–7.0 [5]. Moreover, the choice of the electrode is crucial and will have a large influence on the detection of nitrates. The development of nanoscale materials in recent years has been extensive, particularly with respect to metallic nanoparticles. Interests have focused on their use in analytical chemistry because of their specific physicochemical properties [7,8]. These include enhanced diffusion of electroactive species based on the high effective surface area of metallic nanoparticles improved selectivity, catalytic activity, higher signal-to-noise ratio and unique optical properties [9].These attractive properties favor the appearance of a new kind of electrode modification involving metallic nanoparticles [10].

Therefore, silver nanoparticles AgNPs have been used for electroanalysis applications [11,12]. They have been immobilized on electrode surfaces either through the use of previously prepared Ag colloidal solutions obtained by chemical reduction of silver salts mainly [13,14] or by direct electrochemical deposition on the electrodes, and so on. Several recent works have been published on the synthesis of AgNPs for the electrode modification to detect NO_3^- ions in water at neutral pH [5,15–19]. However, very few of them are based on the *in situ* generation of AgNPs directly functionalized on the electrode surfaces [19,20].

The organometallic route is a useful method employed in our team to obtain small size and narrow dispersion nanoparticles (NPs) stabilized by ligands in organic solution [21–24]. Inspired by the NPs synthesis technique, this work presents an innovative way for the *in situ* functionalization of a gold substrate (E_{Au}) by AgNPs using the hydrogenolysis of a silver metalorganic precursor in liquid phase and mild conditions. We report here for the first time, the *direct* decomposition of N,N′-diisopropylacetamidinate silver precursor ([Ag(Amd)]) in solution without any additional stabilizing ligands for the functionalization of gold substrate by AgNPs ($E_{Au/AgNPs}$).

In our previous work, the electroactvity of the AgNPs electrodeposited on a gold bare disk electrode in sea water seemed even more pronounced in the presence of dissolved oxygen (O_2). As a consequence, the electroactivity of this functionalized gold substrate ($E_{Au/AgNPs}$) has been studied for oxygen reduction reaction (ORR) and the reduction of NO_3^- in aerated sea water. This new electrode has been successfully used for the nanomolar electroanalytical detection of NO_3^- water by square wave voltammetry (SWV) at pH = 6.0.

2. Materials and Methods

2.1. Chemicals

The silver nanoparticles (AgNPs) deposited on gold substrates (electrode surfaces) were obtained by the *in situ* decomposition of N,N′-diisopropylacetamidinate silver precursor ([Ag(Amd)]) in toluene. The synthesis of this silver precursor is described in Section 2.2.

Toluene and Et_2O were obtained from a solvent purification system (Braun) and were further degassed by freeze/pump cycles in a Schlenk vessel. Methyllithium, 1,3-diisopropylcarbodiimide,

and silver chloride were supplied by Sigma Aldrich. All precursors were stored in a glove-box in order to avoid any traces of moisture or air contamination of the chemicals. All experiments were carried out in an argon atmosphere with the exclusion of light, using either glove-box or standard Fischer-Porter techniques. Glassware was oven-dried at 383 K prior to use.

For electrochemical measurements, all the solutions were prepared in Milli-Q water (Millipore Milli-Q water system, 18.2 MΩcm). Standard artificial sea water was prepared from sodium chloride solution (NaCl, EMSURE, supplied by Merck) at 34.5 $g \cdot L^{-1}$ (0.6 $mol \cdot L^{-1}$). This sodium chloride solution was used as a supporting electrolyte. Sulphuric acid solution at 0.5 $mol \cdot L^{-1}$ was used to clean the surfaces of the gold substrates ("bare" gold electrode) and was prepared from H_2SO_4 95% (normapur grade) supplied by VWR Prolabo. A standard nitrate stock solution of $(1.01 \pm 0.01) \times 10^{-6}$ $mol \cdot L^{-1}$ was prepared by dilution of $(1.02 \pm 0.01) \times 10^{-3}$ $mol \cdot L^{-1}$ in artificial sea water solution and then used as it for further dilution. The $(1.02 \pm 0.01) \times 10^{-3}$ $mol \cdot L^{-1}$ nitrate solution was prepared from a suprapure sodium nitrate $Na(NO_3)$.

2.2. Synthesis of N,N′-Diisopropylacetamidinate Silver Precursor ([Ag(Amd)])

The silver amidinate precursor was prepared according to the method described by R. Gordon [25]. A solution of methyllithium (1.6 M in Et_2O, 41 mL, 0.065 mol, 1.2 eq.) in Et_2O was added dropwise to a solution of 1,3-diisopropylcarbodiimide (6.9 g, 0.055 mol) in 100 mL of Et_2O at 243 K. The mixture was warmed to room temperature and stirred for 4 h. This colorless solution was then added to a solution of silver chloride (7.74 g, 0.054 mol) in 50 mL of Et_2O. The reaction mixture stirred during 12 h with the exclusion of light resulted in a black solution. Volatiles solvents were then removed in a vacuum, and the resulting solid is extracted with pentane (100 mL). The pentane extract was filtered through a glass frit (porosity n°3) to result in a pale yellow solution. A concentration of the filtrate followed by cooling to 243 K afforded colorless crystals (75%).

2.3. Gold Substrates (E_{Au}): Gold Electrodes Fabrication

Gold based working electrodes (WE) were fabricated on silicon substrate using metal deposition layers by PVD (Physical Vapour Deposition) at the Laboratoire d'Analyse et d'Architecture des Systèmes (LAAS) facilities. Starting from a conductive boron doped silicon wafer Si (P++), three different metal layers were deposited in a row under secondary vacuum conditions. First, a 20 nm thick titanium underlayer was deposited to ensure the adhesion of the next layer on the substrate. Then, an intermediate 200 nm thick platinum layer was used as a barrier layer for titanium atoms. Finally, a 400 nm thick gold layer or silver layer was deposited to achieve the WE layer. The wafers were finally diced in 8 mm × 8 mm squares that are directly introduced in a specific electrode holder with an electrical connection on the back-side of the Si (P++) silicon substrate.

2.4. In Situ Functionalization of Gold Substrate by AgNPs ($E_{Au/AgNPs}$) and Characterization of $E_{Au/AgNPs}$

The deposition of AgNPs on gold substrate (E_{Au}) was prepared by an adaptation of an original method recently developed in our group [25]. In this pioneering work, a copper amidinate precursor solution was decomposed in H_2 to yield metastable colloidal Cu NPs that undergo a condensation mechanism and eventually form a continuous metallic film on every immersed surface (reactor walls, substrate) [26]. For the Ag NPs deposition process developed in this work, we took advantage of the formation step of colloidal NPs and we use two major parameters to control the condensation of Ag NPs: (1) a low concentration of silver precursor [Ag(Amd)] and (2) a short reaction time to avoid the aggregation of silver on the substrate. No additional stabilizing agent was employed and the silver precursor is directly decomposed in the presence of the working electrode (E_{Au}) placed inside the glass reactor. The key parameter of this process was the contact duration of the substrate with the precursor solution during the hydrogenolysis reaction. The optimized functionalization conditions correspond to a silver precursor concentration of 0.04 $mol \cdot L^{-1}$, and a hydrogenolysis duration of 1 min (Figure 1).

The AgNPs surface density on gold electrode was directly controlled by the hydrogenolysis time on the substrate.

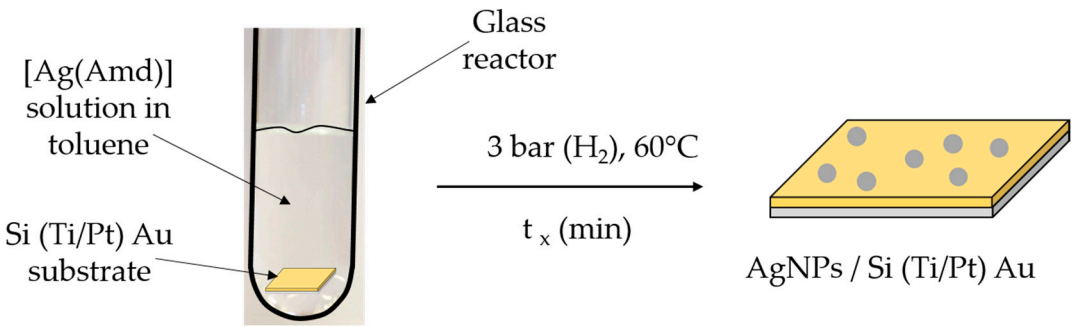

Figure 1. Scheme of the *in situ* deposition of AgNPs by the direct decomposition of [Ag(Amd)] in solution in the presence of the Si(Ti/Pt)Au substrate.

The $E_{Au/AgNPs}$ electrodes were then carefully rinsed using milliQ water before electrochemical reduction of NO_3^- ions and their activation in an artificial sea water (NaCl, pH = 6.0) by running ca. 20 scans between 0.00 V and −1.40 V.

The E_{Au} and $E_{Au/AgNPs}$ electrodes were characterized by field emission gun scanning electron microscopy (FEG-SEM).

2.5. Characterization of Gold Electrode Modified by Silver Nanoparticles ($E_{Au/AgNPs}$)

The FEG-SEM analysis was performed using JEOL JSM-7800F prime equipment with an accelerating voltage of 5 kV and a working distance between 3 and 8 mm depending on the sample. Image analysis was carried out using Image Tool software for the estimation of the average diameter of the silver nanoparticles counting at least a minimum of 100 nanoparticles per image.

2.6. Electrochemical Measurements

All the electrochemical measurements were carried out using a Metrohm potentiostat (PGSTAT 128 N) (Metrohm, Villebon-sur-Yvette, France) interfaced to a laptop computer and controlled with General Purpose Electrochemical System (GPES 4.9) software package (Metrohm). The experiments were carried out at room temperature in a conventional three-electrode cell (Metrohm), with a radiometer saturated calomel reference electrode (SCE) attached to a Luggin capillary and a carbon electrode as counter electrode. Sodium chloride solution at 34.5 $g \cdot L^{-1}$ (0.6 $mol \cdot L^{-1}$) was used as artificial sea water and then as supporting electrolyte. The working electrode E_{Au} or $E_{Au/AgNPs}$ (8 mm × 8 mm) was placed into a radiometer Teflon holder with an effective diameter of 5 mm (area A = 19.6 × 10^{-2} cm^2). The electrochemical cell was maintained in a Faraday cage in order to minimize the electrical interferences.

The oxygen reduction reaction (ORR) was performed by cyclic voltmmetry (CV) in the potential range $-1.3 \leq E\ (V) \leq -0.10$. In order to test and optimize the response of $E_{Au/AgNPs}$ electrodes towards low nitrate ions detection, a series of experiments was performed by CV with different AgNPs deposits (not shown). The optimized functionalization conditions correspond to a silver precursor concentration of 0.04 $mol \cdot L^{-1}$ and a hydrogenolysis duration of 1 min. Further experiments of the electro reduction of nitrate ions was investigated either by square wave voltammetry (SWV) in the potential range $-1.3 \leq E\ (V) \leq -0.10$. This electrochemical method is more sensitive than cyclic voltammetry thanks to short-term square shape potential pulses combined with staircase potential ramp and current sampling allowing a decrease in the contribution of capacitive current. This pulse technique is attractive for quantitative analysis since it leads to better resolved peaks (Gaussian shape) and less distorted by the capacitive current. Indeed, in order to obtain the highest sensitivity (corresponding to the electron (s) transfer), it is important to reduce the effect of the capacitive current

and only measure the contribution of the faradic current. The current (i) is therefore sampled at the end of each potential pulse (forward pulse and backward pulse) as the faradic current decreases slower than the capacitive current with time $\Delta i = i_{pulse\ forward} - i_{pulse\ backward}$ [27,28].

The SWV parameters have been chosen in order to obtain the least noisy signal possible using the classical frequency of f = 100 Hz, an amplitude of E_{SW} = 50 mV and a staircase potential E_{step} = 5 mV. All potentials were reported with respect to the reference electrode (SCE).

3. Results and Discussion

3.1. Characterization of the Gold Electrode Functionalized by Silver Nanoparticles ($E_{Au/AgNPs}$)

Figure 2 shows a typical FEG-SEM image of the deposit of AgNPs obtained by the direct hydrogenolysis of the [Ag(Amd)] organometallic precursor on the gold electrode in liquid phase. The deposit of AgNPs is homogeneous with very well dispersed AgNPs on the gold grains of the electrode which is not totally covered by AgNPs. The AgNPs are very small with an average size of 4 nm. Figure S1 shows a typical FEG-SEM image of a pure gold substrate without AgNPs.

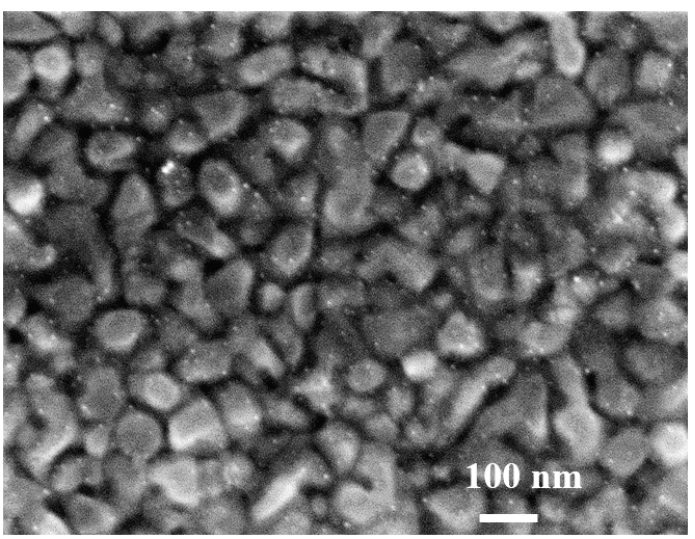

Figure 2. Field emission gun scanning electron microscopy (FEG-SEM) image of the gold electrode functionalized by silver nanoparticles ($E_{Au/AgNPs}$). The functionalization conditions correspond to a silver precursor concentration of 0.04 mol·L^{-1}, and a hydrogenolysis duration of 1 min. The image shows small white dots which represent the very small AgNPs and the Au grains (average size ca. 150 nm) of the gold electrode (E_{Au}).

3.2. Cyclic Voltammetry for the Oxygen Reduction Reaction ORR and the Electroreduction of NO_3^- Ions

The importance of H_2O_2 species in the catalytic process of the NO_3^- electro reduction at a bare gold electrode modified by electrodeposited AgNPs has been shown in a previous work [19]. So, it has been important to observe first the behavior of the modified gold electrode by AgNPs obtained by the hydrogenolysis of [Ag(Amd)] precursor decomposition on ORR without any nitrate ions in the solution (Figure 3A). The ORR on $E_{Au/AgNPs}$ occurs in two steps at −0.4 V (first step) and −0.6 V (second step). However, even if the ORR occurs in two steps at −0.4 V (first step) and −0.6 V (second step), the number of electrons involved in the first step in unusual as it is near three. Indeed, it is well admitted that ORR follows two consecutive reactions through two-electron processes on E_{Au} according to reactions (1) and (2) [29,30], whereas it is consistent with a four-electron transfer on AgNPs according to reaction (3) [13,31]:

$$O_2 + 2H^+ + 2e^- \rightarrow H_2O_2 \quad (1)$$

$$H_2O_2 + 2H^+ + 2e^- \rightarrow 2H_2O \quad (2)$$

$$O_2 + 4H^+ + 4e^- \rightarrow 2H_2O \quad (3)$$

In consequence, the shape of the CVs obtained on $E_{Au/AgNPs}$ (Figure 3A) results probably from the combination of the two mechanisms. Prior studies have shown that Ag surfaces display a better catalytic activity for ORR than a gold one because of its stronger oxygen binding energy. The ORR activity was further enhanced when both Ag and Au surfaces were exposed and accessible due to synergetic interactions between the two metals, certainly by a charge transfer from Au to Ag that inhibits the formation of silver oxide inactive for ORR in the pH conditions [32–34].

In this study, the peak at −0.6 V (i_{pc}) observed during the forward scan on $E_{Au/AgNPs}$ and the absence of peak during the backward scan reveal the irreversibility of the ORR system. These results are predicted by Equation (4) [28]:

$$i_{pc} = 2.99 \times 10^5 \alpha^{1/2} A D^{1/2} \upsilon^{1/2} C^* \quad (4)$$

where α cathodic transfer coefficient, A: electrode area (cm^2), D: diffusion coefficient ($cm^2 \cdot s^{-1}$), C*: concentration of oxygen in the solution ($mol \cdot cm^{-3}$). D was already estimated to be 9.0×10^{-6} $cm^2 \cdot s^{-1}$ [18], the oxygen solubility ($SO_2 = 2.06 \times 10^{-4}$ $mol \cdot L^{-1}$) in sea water (Patm.) [30].

The comparison of the results obtained with electrodeposited AgNPs [19] and the present work indicates that there is a change in the ORR mechanism. Moreover, the current densities calculated for the same experimental conditions (oxygen concentration, sweep rate) is 75 times higher with AgNPs obtained by the metalorganic deposition. This electrocatalytic effect is mainly due to the increase of the surface resulting from small and well dispersed AgNPs on the gold substrate (E_{Au}). The nanostructuration of gold substrate with AgNPs strongly influences the electrode surface and then the electroactivity of nitrate ions.

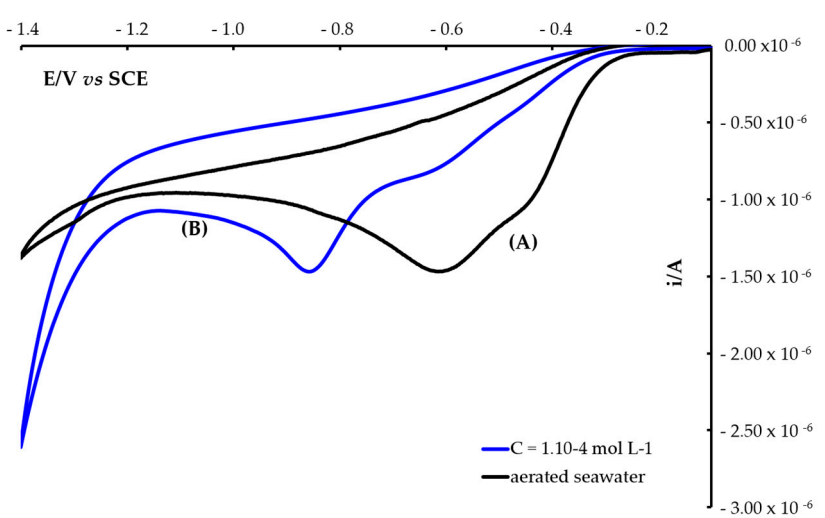

Figure 3. Cyclic voltammograms of aerated artificial sea water on functionalized gold electrode by AgNPs obtained by metalorganic deposition ($E_{Au/AgNPs}$) without nitrate (**A**) and with nitrate [NO_3^-] = 10^{-4} $mol \cdot L^{-1}$ (**B**). Start potential −0.10 V and end potential −1.3 V. Artificial sea water, [NaCl] ~0.6 $mol \cdot L^{-1}$; pH = 6.0, scan rate: 0.100 $V \cdot s^{-1}$. $V_{solution}$ = 10 mL.

The Figure 3B represents the CV on $E_{Au/AgNPs}$ after the addition of 10 $^{-4}$ $mol \cdot L^{-1}$ of NO_3^- ions into the sea water electrolyte. The presence of NO_3^- hinders the ORR in the potential range $-0.6 < E\ (V) < -0.3$ V and leads to a reduction peak of NO_3^- at −0.85 V (Figure 3B). This potential is about 250 mV higher than in the case of electrodeposited Ag, i.e., −1.1 V. This indicates the remarkable electro catalytic properties of the metalorganic-based AgNPs deposited on the gold

electrode ($E_{Au/AgNPs}$). Adsorption times for NO_3^- depends of the size of the nanoparticles, of the diffusion coefficient and of the concentration. The analytical model developed by Compton indicates that for small NPs (<10 nm) a surface coverage with NO_3^- higher than 30% may be reached in less than a second for very low concentrations (<50 nM) [35]. Consequently, when the CV experiment begins it is assumed that NO_3^- species are already adsorbed on the electrode surface. DFT calculations of the absorption energy of NO_3^- on various surfaces allowing on foresee the surface presenting the highest electro catalytic activity for their reduction. These theoretical calculations were experimentally verified by sub-monolayers amounts of Ag deposited on polycrystalline gold electrode [36].

The following detection mechanism based on a mono electronic reduction of NO_3^- followed by a disproportionation on Ag clusters according to the reaction (5) was proposed [19]:

$$H_2O + 2NO_2 \rightarrow NO_3^- + NO_2^- + 2H^+ \quad (5)$$

This electro catalytic reaction occurs simultaneously with the oxidation of NO_2^- and H_2O_2 resulting of the bi electronic transfer for ORR on E_{Au} (see reactions (1) and (2), respectively):

$$H_2O_2 + NO_2^- \rightarrow NO_3^- + H_2O \quad (6)$$

The ratio of the density currents peaks for the NO_3^- reduction by CVs is about 750 times higher when metalorganic-based AgNPs are used instead of electrodeposited AgNPs (not shown). This result confirms the efficiency of the organometallic approach for the grafting of small (<10 nm) and high surface/volume ratio AgNPs on gold surface. The high ratio of the peak currents suggests that the surface of AgNPs is very favorable to the electro reduction of NO_3^- by cyclic voltammetry (Figure 3B and Figure S2). This is due to the catalytic activity of the electrode both for ORR and nitrate reduction. As a matter of fact, the rate of the reaction (6) is increased because of the good performance of the electrode for the ORR reaction and a higher H_2O_2 concentration. However, it has not been possible to achieve the detection of NO_3^- at a level lower than 10^{-6} mol·L^{-1} (Figure S2) by CV in these conditions [37]. In order to improve the limit of detection (LOD) of the device, we have set up the square wave voltammetry (SWV) to the following experiments.

3.3. Analytical Performances towards Nitrate Ions NO_3^- Concentration by Square Wave Voltammetry (SWV)

SWV is an electrochemical method with a short time response, high sensitivity, and high selectivity [27,28]. The better sensitivity results from the minimization of the capacitive current compared with the faradaic current; such a rejection of the background current enables the method to be competitive with other pulse voltammetries. Figure 4 shows the voltammograms obtained with $E_{Au/AgNPs}$ electrode. Successive amounts of NO_3^- ions (1.0×10^{-9} mol·L^{-1}) were added to the sea water solution (34.5 g·L^{-1} NaCl) for NO_3^- ions concentrations and the corresponding SWV were recorded. A first peak at −0.5 V is observed. When a very low nitrate concentration is added this peak current slightly decreases and a second one, centered at −0.8 V, appears. The first peak at −0.5 V is correlated to the ORR and the second one to the NO_3^- reduction in good agreement with the previously suggested mechanism [19]. Importantly, the peak at −0.8 V increases with the nitrate concentration key point for the analytic application. This confirms the remarkable electro catalytic properties of the metalorganic-based AgNPs deposited on the gold electrode (E_{Au}/AgNPs). Moreover, the square wave voltammograms on E_{Au} electrode in aerated artificial seawater with and without nitrate ions are reported on Figure S3. It clearly shows that the "bare" Au electrode (E_{Au}) is not responsible of the electroreduction of NO_3 ions as there is no peak in the range −0.60–1.20 V. However, there is an electrochemical response corresponding to the oxygen reduction which occurs in two steps at −0.4 V (first step) and −0.6 V (second) as it has been already observed previously [19].

Under the optimized experimental conditions (see SWSV parameters as described in Section 2.6), the calibration curve obtained on the $E_{Au/AgNPs}$ electrode exhibits a good linearity in the range 10.0–1.0 nM (10 standard concentrations) with a correlation coefficient R^2 of 0.9931. From the slope of

the calibration plot, the sensitivity of the $E_{Au/AgNPs}$ electrode was found to be 12 μA(mmol·L^{-1})$^{-1}$ (Figure 4, inset). The resulting limit of detection (LOD) is of 0.9 nmol·L^{-1}. To the best of our knowledge, such a performance is the best obtained for electrochemical NO_3^- ions determination in "sea water". The performance using different Ag based electrochemical NO_3^- sensors reported in the literature is compared to our results is shown in Table 1.

Start potential −0.10 V and end potential −1.3 V with a scan frequency of 100 Hz, an amplitude of E_{SW} = 50 mV and a staircase potential E_{step} = 5 mV, [NaCl] ~0.6 mol·L^{-1}; pH = 6.0. $V_{solution}$ = 10 mL. From top to bottom: 1.0, 2.0, 3.0, 4.0, 5.0, 6.0, 7.0, 8.0, 9.0 and 10.0 nmol·L^{-1} NO_3^-, respectively.

This bibliographic survey highlights that these results are mainly obtained by electrodeposition of silver salt precursors. In this case, the best limit of quantification (LOQ) which has been obtained is 0.39 μmol·L^{-1} in a chloride solution in the concentration range (0.39–50 μmol·L^{-1}) with a Au electrode with an optimal charge for AgNPs electrodeposition [5]. Evident is the remarkable increase of the analytical performance of several orders of magnitude due to the combination of the gold electrode modified by AgNPs generated *in situ* by the direct hydrogenolysis of 0.04 mol·L^{-1} [Ag(Amd)] with a duration of 1 min. The combination of E_{Au} and AgNPs is the optimized combination for the electro reduction of NO_3^- ions at very low concentration in artificial sea water. The morphology, size, and surface repartition of these metalorganic-based AgNPs are key parameters for a very performant detection of NO_3^- at very low concentration. Their dispersion and properties on the gold electrode are certainly favorable to the adsorption of NO_3^- ions close enough to hydrogen peroxide production to ensure an optimal chemical reaction.

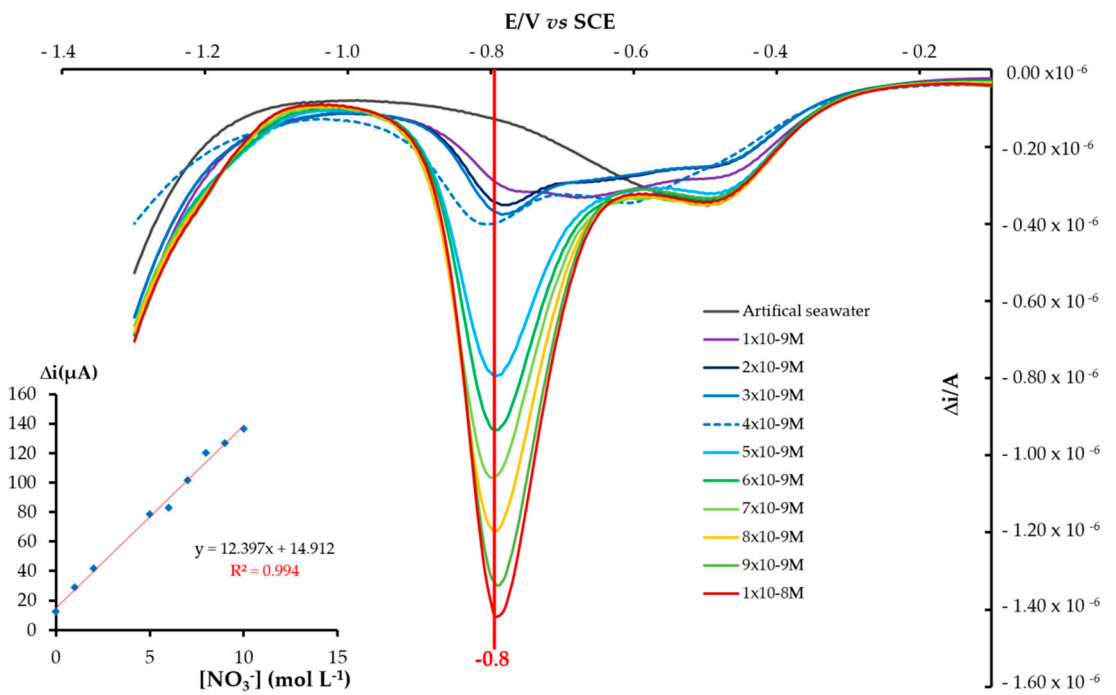

Figure 4. Square wave voltammograms obtained in aerated artificial seawater for succesive nirate ions concentrations on the gold electrode functionalized by *in situ* metalorganic deposition of silver nanoparticles ($E_{Au/AgNPs}$). Inset: Calibration plot based on the peak current (Δi). i vs. [NO_3^-] and linear regression.

Table 1. Comparison of electrochemical sensors based on silver nanostructure for nitrate determination.

Nanostructure	Preparation	Electrolyte	pH	Method	Linear Range (μM)	Sensitivity ($\mu A \cdot mM^{-1} \cdot cm^{-2}$)	LOD LOQ (μM)	References
3D Ag Array	Electrodeposition	0.5M NaCl	7.0	SWV	2–1000	28.2	2	[15]
Ag NPs/C	Electrodeposition	0.1M Na_2SO_4	6.5	Amp.	4–1000	Not indicated	3.2	[16]
Ag NPs/Graphite sheets	Electrodeposition	Phosphate buffer	6.7	Amp.	20–5000	1700	10	[17]
Ag NPs/GC	Electrodeposition	Phosphate buffer	6.7	Amp.	10–5000	3400	4	[17]
Ag NPs/Au	Electrodeposition	0.6M NaCl	6.0	CV	10–1000	3000	10	[19]
Ag NP/polypyrrole/GC	Electrodeposition	0.1M KCl	7.0	DPV	1–10000	2500	2	[18]
Ag NPs/Iron oxide	Chemical	Phosphate buffer	7.0	Amp.	0–1000	660	30	[19]
Ag NPs/Au	Electrodeposition	0.6M NaCl	6.0	SWV	0.39–50	Not indicated	0.39	[5]
Ag NPs/Au	Metalorganic	0.6M NaCl	6.0	SWV	0.9×10^{-3}–1000	5000	0.9×10^{-3}	This work

GC: glassy carbon; SWV: square wave voltammetry; Amp.: amperometry; CV: cyclic voltammetry; DPV: differential pulse voltammetry.

4. Conclusions

In this work we have presented the very first silver nanoparticles based sensor able to detect NO_3^- in artificial sea water, by square wave voltammetry, at a level as low as 0.9 nmol·L^{-1}. This performance results from two different chemical reactions coupled to the electron transfer during the electro-reduction of NO_3^-. On one hand, we observe the disproportion of nitrogen dioxide radicals on Ag NPs deposited on a gold electrode. On the other hand, the spontaneous reaction between hydrogen peroxide produced on a gold surface with nitrite, coming from the reduction of NO_3^- on AgNPs, is responsible for the exaltation of the electro-catalytic current. Besides the analytical application, such electro-catalytic properties of the presented AgNPs-modified Au electrode, could be exploited in a future research work both for NO_3^- reduction and ORR in neutral media (continental waters or health applications).

Supplementary Materials: The following are available online at http://www.mdpi.com/2227-9040/6/4/50/s1, Figure S1: FEG-SEM image of the gold substrate without silver nanoparticles (E_{Au}) and with silver nanparticles obtained with of [Ag(amd)] = 0.04 mol·L^{-1}, duration of [Ag(amd)] decomposition = 1 min. Figure S2: Cyclic voltammograms of aerated artificial sea water on functionalized gold electrode by AgNPs obtained by metalorganic deposition with the optimized conditions, without nitrate ions (A) and with nitrate ions with successive amounts of 10^{-1} mol·L^{-1} in artificial sea water. The concentration range of [NO_3^-] is comprised $10^6 \leq$ [NO_3^-] $\leq 10^{-4}$ mol·L^{-1} (B). Start potential −0.10 V and end potential −1.3 V. Artificial sea water, [NaCl] ~0.6 mol·L^{-1}; pH = 6.0, scan rate: 0.100 V·s^{-1}. Figure S3: Square wave voltammograms of aerated artificial sea water on bare gold electrode wihtout nitrate ions (A) and with nitrate ions, [NO_3^-] = 10^{-3} mol·L^{-1} (B). Start potential −0.10 V and end potential−1.3 V. Artificial sea water, [NaCl] ~0.6 mol·L^{-1}; pH 6.0, scan rate: 0.100 V·s^{-1}.

Author Contributions: Conceptualization, K.F. and M.C.; Methodology, P.F., K.F. and M.L.K.; Substrates, P.T.-B.; Software, A.S.-S., B.D.; Validation, A.S.-S.; Formal Analysis, P.B. and E.L.; Investigation, E.L.; Resources, M.L.K.; Data Curation, E.L. and Writing-Original Draft Preparation, M.C. and K.F.; Writing-Review & Editing, K.F., P.F. and E.L.; Visualization, Supervision, K.F., P.F.; Project Administration, B.D.; Funding Acquisition, P.B.

Acknowledgments: This work was supported by the MIACTIS project: "Microsystèmes intégrés pour l'analyse des composés en traces in situ" (Integrated microsystems for the analyses of in situ trace compounds) as part of the overall project "Instrumentation and Environmental Sensors" funded by the RTRA-STAE: thematic network of the foundation for scientific cooperation "Sciences et Technologies pour l'Aéronautique et l'Espace" (Sciences and Technologies for Aeronautic and Space) in Toulouse, France. This work was partially supported by LAAS-CNRS micro/nano-technologies platform, member of the French RENATECH network and the EquipEX CRITEX. The authors wish to acknowledge the financial support of the Centre National de la Recherche Scientifique (CNRS). The authors acknowledge Vincent Collière for his precious help in SEM-FEG. The authors also thank the reviewers for their useful comments.

Conflicts of Interest: The authors declare no conflict of interest.

References

1. Moorcroft, M.J.; Davis, J.; Compton, R.G. Detection and determination of nitrate and nitrite: A review. *Talanta* **2001**, *54*, 785–803. [CrossRef]
2. Solail, M.; Adeloju, S.B. Nitrate biosensors and biological methods for nitrate determination. *Talanta* **2016**, *153*, 83–98. [CrossRef] [PubMed]
3. Patey, M.J.; Rijkenberg, M.J.A.; Statham, P.J.; Stinchcombe, M.C.; Achterberg, E.P.; Mowlen, M. Determination of nitrate and phosphate in sea water at nanomolar concentrations. *Trends Anal. Chem.* **2008**, *27*, 169–182. [CrossRef]
4. Wang, Q.-H.; Yu, L.-J.; Liu, Y.; Lin, L.; Lu, R.; Zhu, J.; He, L.; Lu, Z.-L. Methods for the detection and determination of nitrite and nitrate: A review. *Talanta* **2017**, *165*, 709–720. [CrossRef] [PubMed]
5. Chen, L.D.; Barus, C.; Garçon, V. Square Wave Voltammetry Measurements of Low Concentrations of Nitrate Using Au/AgNPs Electrode in Chloride Solutions. *Electroanalysis* **2017**, *29*, 2882–2887. [CrossRef]
6. Rosca, V.; Duca, M.; de Groot, M.T.; Koper, M.T.M. Nitrogen cycle electrocatalysis. *Chem. Rev.* **2009**, *109*, 2209–2244. [CrossRef] [PubMed]
7. Hezard, T.; Fajerwerg, K.; Evrard, D.; Collière, V.; Behra, P.; Gros, P. Influence of the gold nanoparticles electrodeposition method on Hg(II) trace electrochemical detection. *Electrochim. Acta* **2012**, *73*, 15–22. [CrossRef]

8. Liu, Y.; Su, G.; Zhang, B.; Jiang, G.; Yan, B. Nanoparticle-based strategies for detection and remediation of environmental pollutants. *Analyst* **2011**, *136*, 872–877. [CrossRef] [PubMed]
9. Welch, C.M.; Compton, R.G. The use of nanoparticles in electroanalysis: A review. *Anal. Bioanal. Chem.* **2006**, *384*, 601–619. [CrossRef] [PubMed]
10. Campbell, F.W.; Compton, R.G. The use of nanoparticles in electroanalysis: An updated review. *Anal. Bioanal. Chem.* **2010**, *396*, 241–259. [CrossRef] [PubMed]
11. Tashkhourian, J.; Hormozi Nezhad, M.R.; Khodavesi, J.; Javadi, S. Silver nanoparticles modified carbon nanotube paste electrode for simultaneous determination of dopamine and ascorbic acid. *J. Electroanal. Chem.* **2009**, *633*, 85–91. [CrossRef]
12. Baghayeri, M.; Mahdavi, B.; Hosseinpor, Z.; Abadi, M.; Farhadi, S. Green synthesis of silver nanoparticles using water extract of Salvia leriifolia: Antibacterial studies and applications as catalysts in the electrochemical detection of nitrite. *Appl. Organomet. Chem.* **2018**, *32*, 4057. [CrossRef]
13. Liu, M.; Chen, W.W. Green synthesis of silver nanoclusters supported on carbon nanodots: Enhanced photoluminescence and high catalytic activity for oxygen reduction reaction. *Nanoscale* **2013**, *5*, 12558–12564. [CrossRef] [PubMed]
14. Chen, Y.P.; Zhao, Y.; Qiu, K.Q.; Chu, J.; Yu, H.Q.; Liu, G.; Tian, Y.C.; Xiong, Y. Fabrication of dendritic silver nanostructure using an integration of holographic lithography and electrochemical deposition. *Electrochim. Acta* **2011**, *56*, 9088–9094. [CrossRef]
15. Hu, J.; Sun, I.; Bian, C.; Tong, J.; Shanhong, X. 3D Dendritic Nanostructure of Silver-Array: Preparation, Growth Mechanism and Application in Nitrate Sensor. *Electroanalysis* **2013**, *25*, 546–556. [CrossRef]
16. Lotfi, H.R.; Zhad, Z.; Lai, R.Y. Comparison of nanostructured silver-modified silver and carbon ultramicroelectrodes for electrochemical detection of nitrate. *Anal. Chim. Acta* **2015**, *892*, 153–159. [CrossRef] [PubMed]
17. Guadagnini, L.; Tonelli, D. Carbon electrodes unmodified and decorated with silver nanoparticles for the determination of nitrite, nitrate and iodate. *Sens. Actuators B* **2013**, *188*, 8069–8814. [CrossRef]
18. Ghanbari, K. Silver Nanoparticles Dispersed in Polypyrrole Matrixes Coated on Glassy Carbon Electrode as a Nitrate Sensor. *Anal. Bioanal. Electrochem.* **2013**, *5*, 46–58.
19. Fajerwerg, K.; Ynam, V.; Chaudret, B.; Garçon, V.; Thouron, D.; Comtat, M. An original nitrate sensor based on silver nanoparticles electrodeposited on a gold electrode. *Electrochem. Commun.* **2010**, *12*, 1439–1441. [CrossRef]
20. Bonyani, M.; Mirzaei, A.; Leonardi, S.G.; Bonavita, A.; Neri, G. Electrochemical Properties of Ag@iron Oxide Nanocomposite for Application as Nitrate Sensor. *Electroanalysis* **2015**, *27*, 2654–2662. [CrossRef]
21. Chaudret, B. Organometallic approach to nanoparticles synthesis and self organization. *C. R. Acad. Sci Phys.* **2005**, *6*, 117–131. [CrossRef]
22. Debouttiere, P.J.; Coppel, Y.; Behra, P.; Chaudret, B.; Fajerwerg, K. One pot organometallic synthesis of well-controlled gold nanoparticles by gas reduction of Au(I) precursor. A spectroscopic NMR study. *Gold Bull.* **2013**, *46*, 291–398. [CrossRef]
23. Amiens, C.; Chaudret, B.; Ciuculescu-Pradines, D.; Collière, V.; Fajerwerg, K.; Khan, M.L.; Maisonnat, A.; Soulantica, K.; Philippot, K. Organometallic approach for the synthesis of nanostructures. *New J. Chem.* **2013**, *37*, 3374–3401. [CrossRef]
24. Cure, J.; Coppel, Y.; Dammak, T.; Fazzini, P.F.; Mlayah, A.; Chaudret, B. Monitoring the Coordination of Amine Ligands on Silver Nanoparticles Using NMR and SERS. *Langmuir* **2015**, *31*, 1362–1367. [CrossRef] [PubMed]
25. Lim, B.S.; Rahtu, A.; Park, J.S.; Gordon, R.G. Synthesis and characterization of volatile,thermally stable, reactive transition metal amidinates. *Inorg. Chem.* **2003**, *42*, 7951–7958. [CrossRef] [PubMed]
26. Cure, J.; Piettre, K.; Sournia-Saquet, A.; Coppel, Y.; Esvan, J.; Chaudret, B.; Fau, P. A novel method for the metallization of 3D silicon induced by metastable copper nanoparticles. *ACS Appl. Mater. Interfaces* **2018**, *10*, 32838–32848. [CrossRef] [PubMed]
27. Mirčeski, V.; Komorsky-Lovrić, S.; Lovrić, M. *Square-Wave Voltammetry: Theory and Application*; Scholz, F., Ed.; Springer: Berlin, Germany, 2007.
28. Bard, A.J.; Faulkner, L.R. *Electrochemical Methods: Fundamental and Applications*, 2nd ed.; Wiley: New York, NY, USA, 2001; ISBN 978-0-471-04372-0.

29. Raj, C.R.; Abdelrahman, A.J.; Ohsaka, J. Gold nanoparticle-assisted electroreduction of oxygen. *Electrochem. Commun.* **2005**, *7*, 888–893. [CrossRef]
30. Rodriguez, P.; Koper, M.T.M. Electrocatalysis on gold. *Phys. Chem. Chem. Phys.* **2014**, *16*, 13583–13594. [CrossRef] [PubMed]
31. Cleve, T.V.; Gibara, E.; Linic, S. Electrochemical Oxygen Reduction Reaction on Ag Nanoparticles of Different Shapes. *ChemCatChem* **2016**, *8*, 256–261. [CrossRef]
32. Singh, P.; Buttry, D.A. Comparison of Oxygen Reduction Reaction at Silver Nanoparticles and Polycrystalline Silver Electrodes in Alkaline Solution. *J. Phys. Chem. C* **2012**, *116*, 10656–10663. [CrossRef]
33. Mott, D.M.; Dao, T.N.A.; Singh, P.; Shankar, C.; Maenosono, S. Electronic transfer as a route to increase the chemical stability in gold and silver core–shell nanoparticles. *Adv. Colloid Interface Sci.* **2012**, *185*, 14–33. [CrossRef] [PubMed]
34. Chen, L.; Deming, C.P.; Peng, Y.; Hu, P.; Stofan, J.; Chen, S. Gold core@silver semishell Janus nanoparticles prepared by interfacial etching. *Nanoscale* **2016**, *30*, 14565–14572. [CrossRef] [PubMed]
35. Käthelhön, E.; Compton, R.G. Nanoparticles in sensing applications: On what timescale do analyte species adsorb on the particle surface? *Analyst* **2014**, *139*, 2411–2415. [CrossRef] [PubMed]
36. Calle-Vallejo, F.; Huang, M.; Henry, J.B.; Koper, M.T.M.; Bandarenka, A.S. Theoretical design and experimental implementation of Ag/Au electrodes for the electrochemical reduction of nitrate. *Phys. Chem. Chem. Phys.* **2013**, *15*, 3196–3202. [CrossRef] [PubMed]
37. Lebon, E.; JCure, J.; Fau, P.; Kahn, M.L.; Lepetit, C.; Fajerwerg, K. Micromolar nitrate electrochemical sensors for sea water analysis with silver nanoparticles modified gold electrode. In Proceedings of the IEEE Nanotechnology Materials and Devices Conference, Toulouse, France, 9–12 October 2016. [CrossRef]